Aerosol size spectra and CCN activity spectra: Reconciling the lognormal, algebraic, and power laws

Vitaly I. Khvorostyanov[1] and Judith A. Curry[2]

[1]   Empirical power law expressions of the form $N_{CCN} = Cs^k$ have been used in cloud physics for over 4 decades to relate the number of cloud condensation nuclei (CCN) and droplets formed on them to cloud supersaturation, s. The deficiencies of this parameterization are that the parameters C and k are usually constants taken from the empirical data and not directly related to the CCN microphysical properties and this parameterization predicts unbounded droplet concentrations at high s. The activation power law was derived in several works from the power law Junge-type aerosol size spectra and parameters C and k were related to the indices of the power law, but this still does not allow to describe observed decrease of the k-indices with s and limited N_{CCN}. Recently, new parameterizations for cloud drop activation have been developed based upon the lognormal aerosol size spectra that yield finite N_{CCN} at large s, but does not explain the activation power law, which is still traditionally used in the interpretation of CCN observations, in many cloud models and some large-scale models. Thus the relation between the lognormal and power law parameterizations is unclear, and it is desirable to establish a bridge between them. In this paper, algebraic and power law equivalents are found for the lognormal size spectra of partially soluble dry and wet interstitial aerosol, and for the differential and integral CCN activity spectra. This allows derivation of the power law expression for cloud drop activation from basic thermodynamic principles (Köhler theory). In the new power law formulation, the index k and coefficient C are obtained as continuous analytical functions of s and expressed directly via parameters of aerosol lognormal size spectra (modal radii, dispersions) and physicochemical properties. This approach allows reconciliation of this modified power law and the lognormal parameterizations and their equivalence is shown by the quantitative comparison of these models as applied to several examples. The advantages of this new power law relationship include bounded N_d at high s, quantitative explanation of the experimental data on the k-index and possibility to express $k(s)$ and $C(s)$ directly via the aerosol microphysics. The modified power law provides a framework for using the wealth of data on the C, k parameters accumulated over the past decades, both in the framework of the power law and the lognormal parameterizations.

1.   Introduction

[2]   The power law and lognormal parameterizations of aerosol size spectra and supersaturation activity spectra are widely used in studies of aerosol optical and radiative properties, cloud physics, and climate research. These two kinds of parameterizations exist in parallel, implicitly compete, but their relation is unclear. One of the most important applications of the power and lognormal laws is parameterization of the concentrations of cloud drops N_d and cloud condensation nuclei N_{CCN} (CCN), on which the drops form. They influence cloud optical and radiative properties as well as the rate of precipitation formation. Precise evaluation of N_{CCN} is required, in particular, for correct estimation of anthropogenic aerosol effects on cloud albedo [*Twomey*, 1977] and precipitation [*Albrecht*, 1989].

[3]   The most commonly used parameterization of the concentration of cloud drops or cloud condensation nuclei N_{CCN} on which the drops activate is a power law by the supersaturation s reached in a cloud parcel is

$$N_{CCN}(s) = Cs^k, \tag{1}$$

[1]Central Aerological Observatory, Dolgoprudny, Moscow Region, Russia.
[2]School of Earth and Atmospheric Sciences, Georgia Institute of Technology, Atlanta, Georgia, USA.

which is referred to in the literature as the integral or cumulative CCN activity spectrum. Numerous studies have provided a wealth of data on the parameters k and C for various geographical regions [see, e.g., *Hegg and Hobbs*, 1992; *Pruppacher and Klett*, 1997, Table 9.1, hereafter referred to as PK97]. Parameterizations of the type (1) were derived by *Squires* [1958] and *Twomey* [1959], using several assumptions and similar power law for the differential CCN activity spectrum, $\varphi_s(s)$

$$\varphi_s(s) = dN_{CCN}/ds = Cks^{k-1}. \tag{2}$$

Equations (1) and (2) have been used for several decades in many cloud models with empirical values of k and C that are assumed to be constant for a given air mass [PK97] and are usually constant during model runs.

[4] To explain the empirical dependencies (1) and (2), models were developed of partially soluble CCN with the size spectra of Junge-type power law $f(r) \sim r^{-\mu}$ (total aerosol concentration $N_a \sim r^{-(\mu-1)}$) and the index k was expressed as a function of μ. *Jiusto and Lala* [1981] found a linear relation

$$k = 2(\mu - 1)/3, \tag{3}$$

which implies $k = 2$ for a typical *Junge* index $\mu = 4$, while the experimental values of k compiled in that work varied over the range $0.2–4$. *Levin and Sedunov* [1966], *Sedunov* [1974], *Smirnov* [1978], and *Cohard et al.* [1998, 2000] derived more general power law or algebraic equations for $\varphi_s(s)$ and expressed k as a function of μ and CCN soluble fraction. *Khvorostyanov and Curry* [1999a, 1999b, hereafter referred to as KC99a, KC99b] derived power laws for the size spectra of the wet and interstitial aerosol, for the activity spectra $\varphi_s(s)$, $N_{CCN}(s)$ and for the Angstrom wavelength index of extinction coefficient, and found linear relations among these indices expressed in terms of the index μ and aerosol soluble fraction.

[5] A deficiency of (1) is that it overestimates the droplet concentration at large s and predicts values of droplet concentration that exceeds total aerosol concentration; this occurs because of the functional form of the power law and use of a single value of k. Many field and laboratory measurements have shown that a more realistic $N_{CCN}(s)$ spectrum in log-log coordinates is not linear as it would be with $k = $ const, but has a concave curvature, i.e., the index k decreases with increasing s [e.g., *Jiusto and Lala*, 1981; *Hudson*, 1984; *Yum and Hudson*, 2001]. This deficiency in (1) has been corrected in various ways: (1) by introducing the C-k space and constructing nomograms in this space [*Braham*, 1976]; (2) by constructing $\varphi_s(s)$ that rapidly decreases at high s [*Cohard et al.*, 1998, 2000] or integral empirical spectra $N_{CCN}(s)$ [*Ji and Shaw*, 1998] that yield finite drop concentrations at large s; (3) by considering the decrease in the indices μ, k with decreasing aerosol size [KC99a]; (4) by using a lognormal CCN size spectrum instead of the power law, which yields concave spectra [*von der Emde and Wacker*, 1993; *Ghan et al.*, 1993, 1995, 1997; *Feingold et al.*, 1994; *Abdul-Razzak et al.*, 1998; *Abdul-Razzak and Ghan*, 2000; *Nenes and Seinfeld*, 2003; *Rissman et al.*, 2004; *Fountoukis and Nenes*, 2005]. On the basis of these studies, the prognostic equations for the drop concentration are recently being incorporated into climate models [*Ghan et al.*, 1997; *Lohmann et al.*, 1999].

[6] However, the power laws (1), (2) are still used in many cloud models and in analyses of field and chamber experiments. The relation between the power law and newer lognormal parameterization is unclear. In this paper, a modified power law is derived and its equivalence to the lognormal parameterizations is established. In section 2, a model of mixed (partially soluble) dry CCN is developed with parameterization of the soluble fraction as a function of the dry nucleus radius and a power law Junge-type representation of the lognormal size spectra is derived. To allow a more accurate estimate of aerosol contribution into the cloud optical properties and to the Twomey effect, a lognormal spectrum of the wet interstitial aerosol is found using Köhler theory. In section 3, a new algebraic representation of the lognormal spectra is derived. The differential CCN activity spectra as a modification of (2) are derived in section 4 in both the lognormal and algebraic forms. In section 5, the cumulative CCN spectra as a modification of (1) are derived in both lognormal and algebraic forms. Finally, a modified power law is derived as a modification of (1), expressing the parameters C and k as continuous algebraic functions of supersaturation and parameters of aerosol microstructure and physicochemical properties. The advantages of this new power law relationship include drop concentration bounded by the total aerosol concentration at high supersaturations, quantitative explanation of the experimental data on the k-index, and the possibility to express $k(s)$ and $C(s)$ directly via the aerosol microphysics. This formulation allows reconciliation of this modified power law and the lognormal parameterizations, which is illustrated with several examples. Summary and conclusions are given in section 6.

2. Correspondence Between the Lognormal and Power Law Size Spectra

2.1. Lognormal Size Spectra of the Dry and Wet Aerosol

[7] We consider a polydisperse ensemble of mixed aerosol particles consisting of soluble and insoluble fractions. The lognormal size spectrum of dry aerosol $f_d(r_d)$ by the dry radii r_d can be presented in the form:

$$f_d(r_d) = \frac{N_a}{\sqrt{2\pi}(\ln \sigma_d) r_d} \exp\left[-\frac{\ln^2 (r_d/r_{d0})}{2 \ln^2 \sigma_d}\right], \tag{4}$$

where N_a is the aerosol number concentration, σ_d is the dispersion of the dry spectrum, and r_{d0} is the mean geometric radius related to the modal radius r_m as

$$r_m = r_{d0} \exp\left(-\ln^2 \sigma_d\right). \tag{5}$$

As the relative humidity H exceeds the threshold of deliquescence H_{th} of the soluble fraction, the hygroscopic growth of the particles begins and initially dry CCN convert into wet "haze particles." To derive the size spectrum of the wet aerosol, we need relations between the dry radius r_d and a corresponding radius of a wet particle r_w. These relations

can be obtained using the Köhler equation for super-saturation $s = (\rho_v - \rho_{vs})/\rho_{vs}$ that can be written for the dilute solution particles as [PK97]:

$$s = H - 1 = \frac{A_k}{r} - \frac{B}{r^3}. \tag{6}$$

$$A_k = \frac{2M_w \varsigma_{sa}}{RT\rho_w}, \qquad B = \frac{3\nu\Phi_s m_s M_w}{4\pi M_s \rho_w}. \tag{7}$$

Here ρ_v, ρ_{vs}, and ρ_w are the densities of vapor, saturated vapor, and water, H is the ambient relative humidity, A_k is the Kelvin curvature parameter, M_w is the molecular weight of water, ζ_{sa} is the surface tension at the solution-air interface, R is the universal gas constant, T is the temperature (in degrees Kelvin). The parameter B describes effects of the soluble fraction, ν is the number of ions in solution, Φ_s is the osmotic potential, m_s and M_s are the mass and molecular weight of the soluble fraction.

[8] The radius r_w can be related to r_d as in the work of KC99a using a convenient parameterization of the soluble fraction and the parameter B, following *Levin and Sedunov* [1966], *Sedunov* [1974]:

$$B = b r_d^{2(1+\beta)} \tag{8}$$

where the parameters b and β depend on the chemical composition and physical properties of the soluble part of an aerosol particle. The parameter β describes the soluble fraction of an aerosol particle. Generally, the solubility decreases with increasing particle size [e.g., *Laktionov*, 1972; *Sedunov*, 1974; PK97], so that β decreases with increasing r_d and may vary from 0.5, when soluble fraction is proportional to the volume, to -1, when soluble fraction is independent of the radius. This variation describes the change of the dominant mechanisms of accumulation of soluble fraction with growing particle size. A detailed analysis of these mechanisms is given, e.g., in the work of PK97 and *Seinfeld and Pandis* [1998] and is beyond the scope of this paper. We consider in more detail two particular cases.

[9] 1. $\beta = 0.5$. The value $\beta = 0.5$ corresponds to the case $B = b r_d^3$, when soluble fraction is distributed within particle volume, is proportional to it, and is usually implicitly assumed in most parameterizations of CCN deliquescence and drop activation [e.g., *von der Emde and Wacker*, 1993; *Ghan et al.*, 1993, 1995; *Abdul-Razzak et al.*, 1998; *Abdul-Razzak and Ghan*, 2000]. It was found in the work of KC99a that with $\beta = 0.5$, the quantity b is a dimensionless parameter:

$$b = (\nu\Phi_s)\varepsilon_v \frac{\rho_s}{\rho_w} \frac{M_w}{M_s}, \tag{9a}$$

where ρ_s is the density of the soluble fraction, ε_v is its volume fraction.

[10] 2. $\beta = 0$. Then $B = b r_d^2$, i.e., mass of soluble fraction is proportional to the surface area where it is accumulated as a film or shell. The particle volume fraction was parameterized in the work of KC99a as $\varepsilon_v(r_d) = \varepsilon_{v0}(r_{d1}/r_d)$, where

r_{d1} is some scaling parameter and ε_{v0} is the reference soluble fraction (dimensionless). We then obtain for b

$$b = r_{d1}\varepsilon_{v0}(\nu\Phi_s) \frac{\rho_s}{\rho_w} \frac{M_w}{M_s}. \tag{9b}$$

For this case, b has the dimension of length and is proportional to the scaling radius r_{d1}. If the thickness l_0 of the soluble shell is much smaller than the radius r_d of a spherical insoluble core, $l_0 \ll r_d$, then approximately $m_s \approx 4\pi\rho_s r_d^2 l_0$, $\varepsilon_v(r_d) = 3l_0/r_d$, and in (9b) $\varepsilon_{v0} = 1$, $r_{d1} = 3l_0$, and

$$b = 3l_0(\nu\Phi_s) \frac{\rho_s}{\rho_w} \frac{M_w}{M_s}. \tag{9c}$$

The parameterizations (9b) and (9c) might be used, in particular, for surface-active substances that are accumulated near the particle surface [e.g., *Rissman et al.*, 2004] or for soluble shell coatings of particles with insoluble cores such as dust when heterogeneous chemical reactions on the particle surface may lead to formation of such coatings [e.g., *Laktionov*, 1972; *Levin et al.*, 1996; *Sassen et al.*, 2003; *Bauer and Koch*, 2005].

[11] The values of b for aerosols with volume-proportional soluble components ($\beta = 0.5$) consisting of NaCl and ammonium sulphate evaluated from (9a) are determined as follows, using data obtained from PK97. If the soluble material is NaCl ($M_s = 58.5$, $\rho_s = 2.16$ g cm^{-3}, $\nu = 2$, $\Phi_s \approx 1$ for dilute solutions), then $b = 1.33$ for $\varepsilon_v = 1$ (fully soluble nuclei), and $b = 0.26$ for $\varepsilon_v = 0.20$. If the soluble material is ammonium sulphate ($M_s = 132$, $\rho_s = 1.77$ g cm^{-3}, $\nu = 3$, $\Phi_s \approx 0.767$ for molality of 0.1, so that $\nu\Phi_s \approx 2.3$), then $b = 0.55$ for fully soluble nuclei ($\varepsilon_v = 1$), and $b = 0.25$ for $\varepsilon_v = 0.45$. In the calculations below, we consider mostly the case $\beta = 0.5$ (volume-proportional) and use the value $b = 0.25$, which may correspond to the dry aerosol containing $\sim 50\%$ ammonium sulphate, as found by *Hänel* [1976] in measurements of continental and marine (Atlantic) aerosols, or 20% NaCl, as was assumed by *Junge* [1963]. All of the results below can be recalculated for $\beta = 0$ with an appropriate model of the soluble shell (some estimates are given below for the case $\beta = 0$), to any other ε_v, or for any other chemical composition using appropriate values of M_s and ρ_s. The soluble aerosol fraction often decreases with increasing radius [PK97], and this feature can be described by choosing an appropriate superposition of the aerosol size spectra with the two soluble fractions: volume-proportional ($\beta = 0.5$ for smaller fraction) and surface-proportional ($\beta = 0$ for larger fraction).

[12] The size spectrum of the wet aerosol $f_w(r_w)$ can be obtained using the relations between the dry r_d and wet r_w radii. Various solutions for the humidity dependence of $r_w(H)$ at subsaturation and supersaturation were found in algebraic and trigonometric forms using the Kohler's equation (6) [e.g., *Levin and Sedunov*, 1966; *Sedunov*, 1974; *Hänel*, 1976; *Fitzgerald*, 1975; *Smirnov*, 1978; *Fitzgerald et al.*, 1982; *Khvorostyanov and Curry*, 1999a; *Cohard et al.*, 2000]. In this work, we consider only the wet interstitial aerosol, and humidity transformations at subsaturation will be considered in a separate paper.
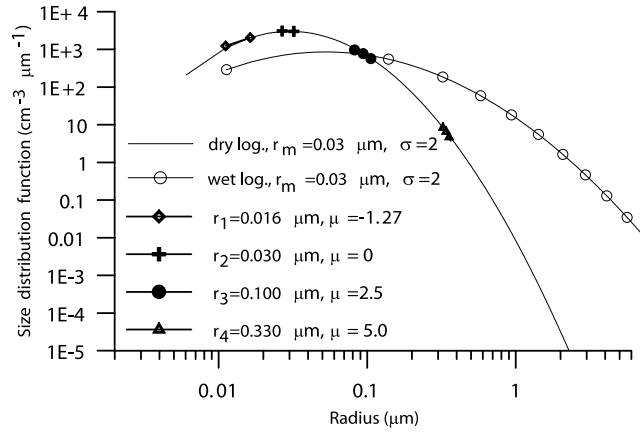
Figure 1. Lognormal dry (solid curve) and interstitial (open circles) aerosol size spectra with the parameters: modal radius $r_m = 0.03$ μm, $\sigma_{d,w} = 2$, $N_a = 200$ cm^{-3}, and the Junge-type power law approximations to the dry spectrum at four points: before modal radius, $r_1 = 0.016$ μm, negative index μ $= -1.27$; modal radius $r_2 = 0.03$ μm, μ $= 0$; $r_3 = 0.1$ μm, μ $= 2.5$; $r_4 = 0.33$ μm, μ $= 5.0$).

[13] The supersaturation in clouds is small ($s \leq 10^{-4}$–10^{-2}), the left-hand side in (6) tends to zero and the radius of a wet particle can be found from the quadratic equation:

$$r_w(H \cong 1) = \left(\frac{B}{A_k}\right)^{1/2} = \frac{b^{1/2}r_d^{1+\beta}}{A_k^{1/2}}. \qquad (10)$$

[14] This expression can be used at the stage of cloud formation (CCN activation into the drops) or for interstitial unactivated cloud aerosol. Now the size spectrum $f_w(r_w)$ can be found from the conservation equation

$$f_w(r_w)dr_w = f_d(r_d)dr_d. \qquad (11)$$

Using (10)–(11), we obtain that the dry distribution (4) transforms into the wet spectrum

$$f_w(r_w) = \frac{N_a}{\sqrt{2\pi}(\ln \sigma_w)r_w} \exp\left[-\frac{\ln^2 (r_w/r_{w0})}{2\ln^2 \sigma_w}\right]. \qquad (12)$$

The wet mean geometric radii r_{w0} and dispersions σ_w are related to the corresponding r_{d0} and σ_d of the dry aerosol as

$$r_{w0} = r_{d0}^{(1+\beta)}(b/A_k)^{1/2}, \quad \sigma_w = \sigma_d^{(1+\beta)}, \quad H \cong 1, \qquad (13)$$

[15] Thus the shape of the wet interstitial size spectrum (12) is the same lognormal as for the dry aerosol (4) but the values of r_{w0} and σ_w are different. The size spectra of the interstitial aerosol at $s > 0$ are limited by the boundary radius $r_b = 2A_k/3s$ [*Levin and Sedunov*, 1966; *Sedunov*, 1974].

2.2. Approximation of the Lognormal Size Spectra by the Junge Power Law

[16] A correspondence between the lognormal and power law size spectra can be established using the same method as in the work of *Khvorostyanov and Curry* [2002, 2005]

for a continuous power law representation of the fall velocities. Suppose $f(r)$ is smooth and has a smooth derivative $f'(r)$. Then they can be presented at a point r as the power law functions

$$f(r) = c_f r^{-\mu}, \quad f'(r) = -\mu f(r)/r \qquad (14)$$

Solving (14) for μ and c_f we obtain:

$$\mu(r) = -\frac{rf'(r)}{f(r)}, \quad c_f(r) = f(r)r^{\mu} \qquad (15)$$

The power index μ and c_f are here the functions of radius. If aerosol size spectrum $f(r)$ is described by the dry $f_d(r_d)$ or wet $f_w(r_w)$ lognormal distributions (4), (12), substitution of $f_{d,w}$ and $f'_{d,w}$ into (15) yields the power index for the dry and wet aerosol spectra

$$\mu_{d,w}(r_{d,w}) = 1 + \frac{\ln(r_{d,w}/r_{d,w0})}{\ln^2 \sigma_{d,w}}, \qquad (16)$$

where the indices "*d, w*" denote dry or wet aerosol, and r_{w0}, σ_{w0} are defined by (14). Thus the lognormal dry and wet spectra (4), (12) can be presented at every point r_d, r_w, in the power law form (14) with the index $\mu_{d,w}$ (16).

2.3. Examples of the Dry and Wet Aerosol Size Spectra and Power Indices

[17] Figure 1 shows in log-log coordinates a lognormal dry aerosol size spectrum $f_d(r_d)$ with modal radius $r_m = 0.03$ μm and dispersion $\sigma_d = 2$, close to *Whitby* [1978] for the accumulation mode, and concentration $N_a = 200$ cm^{-3}. Its Junge-type power law approximations shows the radius dependence of the power index μ: it changes from μ $= -1.27$ at $r_1 = 0.016$ μm $< r_m$, to μ $= 0$ at the modal radius $r_2 = r_m$, and μ is positive at all $r > r_m$; in particular, μ $= 2.5$ at $r_3 = 0.1$ μm and μ $= 5.0$ at $r_4 = 0.33$ μm. Recall that the dimensional analysis of the coagulation equation and its asymptotic solutions yield the inverse power laws with the index μ $= 2.5$ for $r_d \sim 0.1$ μm due to the dominant effects of Brownian coagulation, and μ $= 4.5$ for $r_d > 1$ μm due to prevailing sedimentation [PK97, chap. 11]. The lognormal spectrum with the described parameters is in general agreement with these power law solutions. Thus the lognormal size spectrum can be considered as the superposition of the power laws with the index from (16).

[18] The transition of the dry lognormal spectrum to the limit $H = 1$ (curve with open circles) is fairly smooth, although there is a distinct decrease of the slopes. This resembles a corresponding effect for the power law spectra, when the transition to $H = 1$ is accompanied by a decrease of the Junge power index, e.g., μ $= 4$ at $H < 1$ converts into μ $= 3$ at $H \rightarrow 1$ over a very narrow humidity range [e.g., *Sedunov*, 1974; *Fitzgerald*, 1975; *Smirnov*, 1978; KC99a].

[19] The dependence of the effective power indices calculated for lognormal distributions with various modal radii and dispersions is shown for the dry aerosol in Figure 2, which illustrates the following general features of (16). The indices (the slopes of the spectra) increase with radii for all r. The indices μ increase with decreasing dispersions and with increasing r_{d0} of the dry lognormal spectrum. The
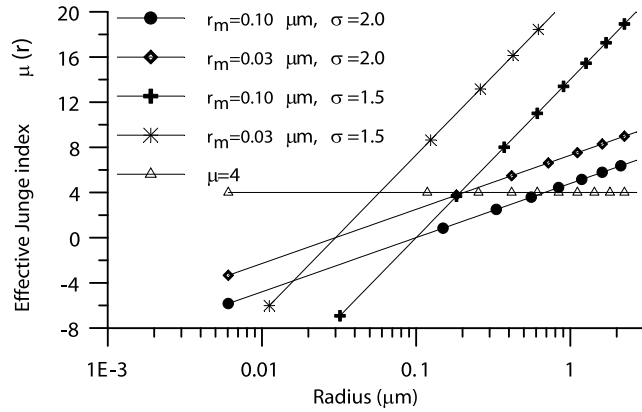
Figure 2. Effective power indices calculated from equation (16) for lognormal distributions with modal radii and dispersions indicated in the legend; the constant value $\mu = 4$ is given for comparison.

calculated μ intersect the average Junge's curve $\mu = 4$ in the range of radii 0.06 μm to 0.7 μm, i.e., mostly in the accumulation mode. Since the values chosen here for r_{d0} and σ_d are realistic (close to Whitby's multimodal spectra), this may explain how a superposition of several lognormal spectra may lead to an "effective average" $\mu = 4$, observed by Junge. The growth of the indices above 4 for larger r is in agreement with the coagulation theory that predicts steeper slopes, $\mu = 19/4$, of the power laws for greater radii $r \geq 5$ μm [PK97]. The described relation between the lognormal and power law size spectra might be useful for analysis and parameterizations of the measured spectra and of solutions to the coagulation equation.

3. Algebraic Approximation of the Lognormal Distribution

[20] A disadvantage of the lognormal size spectra is the difficulty of evaluating analytical asymptotics and moments of this distribution. A convenient algebraic equivalent of the lognormal distribution can be obtained using two representations of the smoothed (bell-shaped) Dirac's delta-function $\delta(x)$. The first one was taken as [*Korn and Korn*, 1968]

$$\delta_1(x, \alpha) = \frac{\alpha}{\sqrt{\pi}} \exp(-\alpha^2 x^2), \tag{17}$$

where α determines the width of the function. Another representation as an algebraic function of $\exp(x/\alpha)$ is given by *Levich* [1969]. We transformed it to the following form:

$$\delta_2(x, \alpha) = \frac{\alpha}{\sqrt{\pi}} \frac{1}{\text{ch}^2(2\alpha x/\sqrt{\pi})}, \tag{18}$$

[21] It can be shown that both functions $\delta_1(x, \alpha)$ and $\delta_2(x, \alpha)$ are normalized to unity, tend to the Dirac's delta-function when $\alpha \to \infty$ and exactly coincide in this limit:

$$\lim_{\alpha \to \infty} \delta_1(x, \alpha) = \lim_{\alpha \to \infty} \delta_2(x, \alpha) = \delta(x). \tag{19}$$

Thus we can use the following equality:

$$\frac{\alpha}{\sqrt{\pi}} \exp(-\alpha^2 x^2) \approx \frac{\alpha}{\sqrt{\pi}} \frac{1}{\text{ch}^2(2\alpha x/\sqrt{\pi})} \tag{20}$$

A comparison shows that both functions are already sufficiently close at values $\alpha \sim 1$, which is illustrated in Figure 3a, where these functions divided by $\alpha/\sqrt{\pi}$ are plotted, the difference generally does not exceed 3–5%. The approximate equality of these smoothed delta functions is used further for an algebraic representation of the aerosol size and CCN activity spectra.

[22] Integration of (20) from 0 to x yields another useful relation:

$$\text{erf}(\alpha x) \approx \tanh(2\alpha x/\sqrt{\pi}), \tag{21}$$

where $\text{erf}(z)$ is the Gaussian function of errors:

$$\text{erf}(z) = \frac{2}{\sqrt{\pi}} \int_0^z e^{-x^2} dx. \tag{21a}$$

Equation (21) with $\alpha = 1$ was found by *Ghan et al.* [1993], who showed its accuracy, which is also illustrated in Figure 3b for two values of α. It is known that integration of the Dirac's delta-function yields Heaviside's step-function. Comparison of Figures 3a and 3b shows that the same is valid for the correspondent smoothed functions, therefore
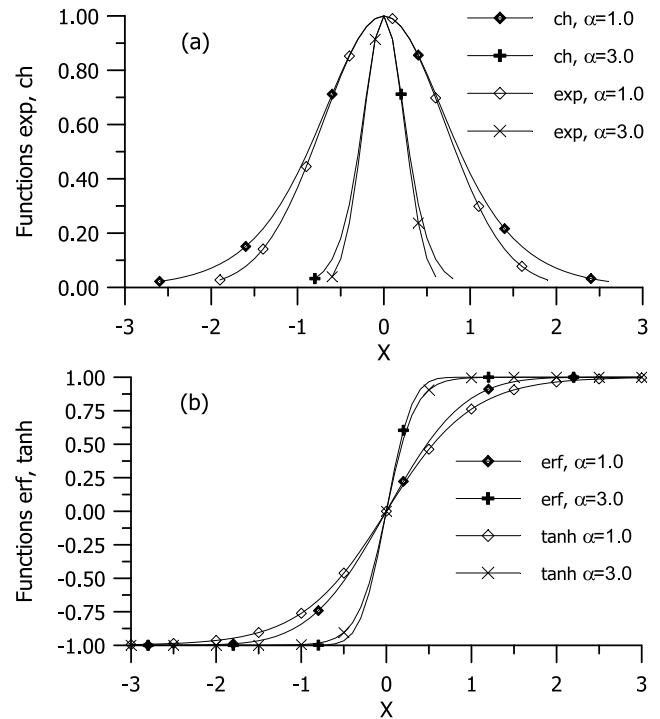

Figure 3. (a) Comparison of the smoothed Dirac delta-functions: $\exp(-\alpha^2 x^2)$, and its approximation $1/\text{ch}^2(2\alpha x/\sqrt{\pi})$, for two values $\alpha = 1$ and 3. The difference generally does not exceed 3–5%. (b) Comparison of the smoothed Heaviside step-functions, $\text{erf}(\alpha x)$, and $\tanh(2\alpha x/\sqrt{\pi})$.
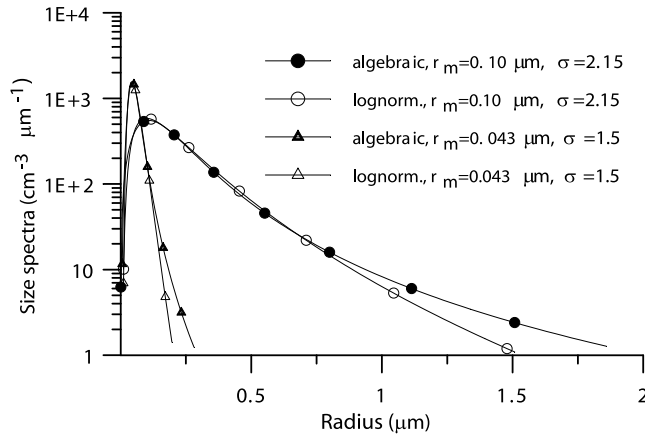
Figure 4. Comparison of the algebraic and lognormal aerosol size spectra for the two pairs of parameters: $r_m = 0.1$ μm, $\sigma_d = 2.15$ (solid and open circles for the algebraic and lognormal, respectively), and $r_m = 0.0.43$ μm, $\sigma_d = 1.5$ (solid and open triangles).

the derivation above shows that the relation (21) is an approximate equality of the two representations of the smoothed Heaviside step-functions. Equation (21) is used in section 5 for the proof of equivalence of the lognormal and algebraic representations of the drop concentration and k-index.

[23] If we introduce in (20) the new variables $x = \ln(r/r_0)$, $\alpha = (\sqrt{2}\ln\sigma)^{-1}$, then $2\alpha x/\sqrt{\pi} = \ln(r/r_0)^{k_0/2}$, where k_0 is a parameter introduced by *Ghan et al.* [1993]:

$$k_0 = \frac{4}{\sqrt{2\pi}\ln\sigma}. \tag{22}$$

Substituting these variables into (20), we obtain

$$\frac{1}{\sqrt{2\pi}\ln\sigma}\exp\left[-\frac{\ln^2(r/r_0)}{2\ln^2\sigma}\right] \approx \frac{k_0(r/r_0)^{k_0}}{\left[(r/r_0)^{k_0}+1\right]^2}. \tag{23}$$

[24] The expression on the left-hand side is the lognormal distribution $dN/d\ln r$ with mean geometric radius r_0 and dispersion σ, and the right-hand side is its algebraic equivalent, which is another representation of the smoothed delta function. When the dispersion tends to its lower limit $\sigma \to 1$, then $\alpha \to \infty$, and according to (19), both distributions tend to the delta function, i.e., become infinitely narrow (monodisperse) at $\sigma = 1$. For $\sigma > 1$, they represent distributions of the finite width. Using the equality (23), the dry (4) and wet (12) lognormal aerosol size spectra can be rewritten in algebraic form as

$$f_d(r_d) = \frac{k_{d0}N_a}{r_{d0}}\frac{(r_d/r_{d0})^{k_{d0}-1}}{\left[1+(r_d/r_{d0})^{k_{d0}}\right]^2}, \tag{24}$$

$$f_w(r_w) = \frac{k_{w0}N_a}{r_{w0}}\frac{(r_w/r_{w0})^{k_{w0}-1}}{\left[1+(r_w/r_{w0})^{k_{w0}}\right]^2}, \tag{25}$$

where r_{d0} and σ_d are the geometric radius and dispersion of the dry spectrum, r_{w0} and σ_w are corresponding quantities for the wet spectrum defined in (13), and the indices k_{0d} and k_{0w} are

$$k_{d0} = \frac{4}{\sqrt{2\pi}\ln\sigma_d}, \quad k_{w0} = \frac{4}{\sqrt{2\pi}\ln\sigma_w}. \tag{26}$$

A comparison of the algebraic (24) and lognormal (4) aerosol size spectra calculated for the two pairs of spectra with the same parameters is shown in Figure 4. One can see that algebraic and lognormal spectra are in a good agreement in the region from the maxima and down by two to three orders of magnitude. A discrepancy is seen in the region of the tails, but this region provides a small contribution into the number density.

[25] These algebraic representations of the size spectra can be useful in applications. Evaluation of their analytical and asymptotic properties is simpler than those of the lognormal distributions, and various moments over the size spectra can be expressed via elementary functions rather than via *erf* as in the case with the lognormal distributions. Being a good approximation to the lognormal distribution but simpler in use, the algebraic functions (24), (25) can be used for approximation of the aerosol, droplet, and crystal size spectra as a supplement or an alternative to the traditionally used power law, lognormal, and gamma distributions. Some applications are illustrated in the next sections.

4. Differential CCN Supersaturation Activity Spectrum

4.1. Critical Supersaturations and Radii

[26] To derive the supersaturation activity spectrum, we need relations among the dry radius r_d, corresponding critical water supersaturation s_{cr}, and the critical nucleus radius r_{cr}. The values r_{cr} and s_{cr} for CCN activation can be found as usually using Köhler's equation (6) from the condition of maximum $ds/dr = 0$:

$$r_{cr} = \left(\frac{3B}{A_k}\right)^{1/2} = r_d^{1+\beta}\left(\frac{3b}{A_k}\right)^{1/2}, \tag{27}$$

$$s_{cr} = \left(\frac{4A_k^3}{27B}\right)^{1/2} = \frac{2}{3}\frac{A_k}{r_{cr}} = r_d^{-(1+\beta)}\left(\frac{4A_k^3}{27b}\right)^{1/2} = c_1^{1/k_1}r_d^{-1/k_1}, \tag{28}$$

where we used again the parameterization (8) for B. These equations can be reverted to express r_d via r_{cr} or s_{cr}:

$$r_d(r_{cr}) = r_{cr}^{k_1}(A_k/3b)^{k_1/2}, \quad r_d(s_{cr}) = c_1 s_{cr}^{-k_1} \tag{29}$$

where

$$k_1 = \frac{1}{1+\beta}, \quad c_1 = \left(\frac{4A_k^3}{27b}\right)^{k_1/2} \tag{30}$$

[27] Figure 5 depicts the critical supersaturations, s_{cr}, and critical radii, r_{cr}, calculated with (27), (28) as functions of r_d
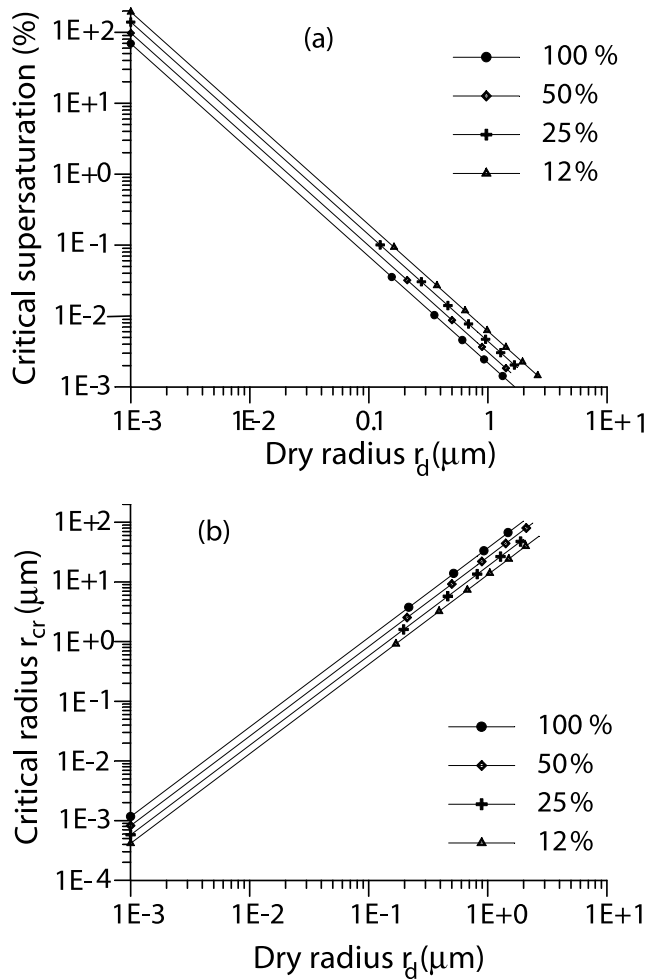
Figure 5. (a) Critical supersaturation, s_{cr}, and (b) critical radius, r_{cr}, calculated as functions of the dry radius r_d with the four values of b corresponding to various soluble fractions of ammonium sulfate indicated in the legend.

with four values of b (0.55, 0.275, 0.135, 0.07), corresponding to various soluble fractions of ammonium sulfate (100, 50, 25, and 12.5%) indicated in the legend. The values of s_{cr} required for activation of a given CCN increase with decreasing r_d from 0.1–0.3% at $r_d = 0.1$ μm (a typical cloud case) to 3–10% at $r_d = 0.01$ μm (as can be found in a cloud chamber) and reach 70–200% at $r_d = 0.001$ μm. The values of r_{cr} increase with r_d and the ratio r_{cr}/r_d reaches 5–13 at $r_d = 0.1$ μm and 13–40 at $r_d = 1$ μm. The 8-fold decrease in the soluble fraction causes s_{cr} to increase and r_{cr} to decrease by a factor of $\sim$3–5.

[28] These features are important for understanding and quantitative description of the separation between activated and unactivated CCN fractions. Figure 6 shows four lognormal size spectra of the dry aerosol with various modal radii and dispersions along with the corresponding critical radii and supersaturations calculated with $\beta = 0.5$, $b = 0.55$ (50% soluble fraction of ammonium sulfate). One can see that if the maximum supersaturation does not exceed $\sim$0.1 %, the right branch of the dry spectrum with $r_m = 0.1$ μm can be activated down to the mode, and the left branch ($r_d < r_m$)

remains unactivated. For the spectrum with $r_m = 0.03$ μm, activation of the right half down to r_m requires a supersaturation of 0.6%. Such a supersaturation is typical of some natural clouds. Activation of the left branches with $r_d < 0.01-0.03$ μm requires higher supersaturations and may be typical of the CCN measurements in cloud chambers where $s \sim 5-20\%$ can be reached [e.g., *Jiusto and Lala*, 1981; *Hudson*, 1984; *Yum and Hudson*, 2001].

4.2. Lognormal Differential CCN Activity Spectrum

[29] The CCN differential supersaturation activity spectrum $\varphi_s(s)$ can be obtained now using the conservation law in differential form for the concentration:

$$f_d(r_d)dr_d = -\varphi_s(s)ds. \tag{31}$$

Here s is the critical supersaturation required to activate a dry particle with radius r_d; the minus sign occurs since increase in r_d ($dr_d > 0$) corresponds to a decrease in s ($ds < 0$) as indicated by (28). Using (29) and (30), (31) can be rewritten in the form:

$$\varphi_s(s) = -f_d(r_d)\frac{dr_d(s)}{ds} = c_2 s^{-k_2} f_d[r_d(s)], \tag{32}$$

where

$$c_2 = \frac{1}{1+\beta}\left(\frac{4A_K^3}{27b}\right)^{1/2(1+\beta)} = k_1 c_1, \quad k_2 = k_1 + 1 = \frac{2+\beta}{1+\beta}. \tag{32a}$$
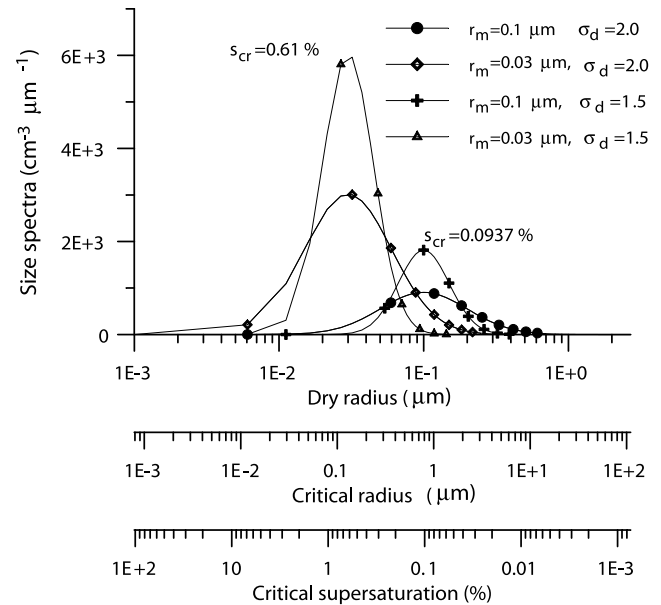

Figure 6. Lognormal aerosol size spectra for $r_m = 0.1$ μm, $\sigma_d = 2$ (solid circles), $r_m = 0.1$ μm, $\sigma_d = 1.5$ (crosses), $r_m = 0.03$ μm, $\sigma_d = 2$ (rhombs), and $r_m = 0.03$ μm, $\sigma_d = 1.5$ (triangles), plotted as the functions of dry radii and of corresponding critical radii and critical supersaturations. Critical supersaturations s_{cr} corresponding to the maxima at 0.1 μm and 0.03 μm are shown near the curves.
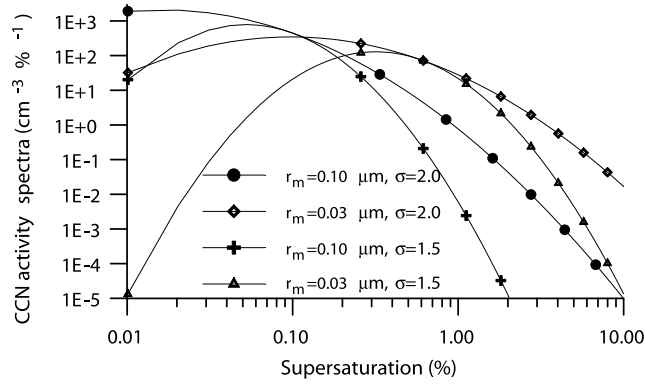
Figure 7. CCN differential activity spectrum $\varphi_s(s)$ calculated with $b = 0.25$ and four combinations of modal radii r_m and dispersions σ_d of the dry aerosol spectra indicated in the legend.

Substituting the dry lognormal size spectrum (4) into (32), we obtain:

$$\varphi_s(s) = \frac{N_a}{\sqrt{2\pi}(\ln \sigma_s)s} \exp\left[-\frac{\ln^2 (s/s_0)}{2 \ln^2 \sigma_s}\right], \qquad (33)$$

where we introduced the mean geometric supersaturation s_0 and the supersaturation dispersion σ_s:

$$s_0 = (r_{d0}/c_1)^{-1/k_1} = r_{d0}^{-(1+\beta)}\left(\frac{4A_k^3}{27b}\right)^{1/2}, \qquad (34)$$

$$\sigma_s = \sigma_d^{1/k_1} = \sigma_d^{(1+\beta)}. \qquad (35)$$

The modal supersaturation s_m is related to s_0 similar to that for the dry size spectrum (5)

$$s_m = s_0 \exp\left(-\ln^2 \sigma_s\right). \qquad (36)$$

The supersaturation activity spectrum (33) has a maximum at s_m and the region $s = s_m \pm \sigma_s$ gives the maximum contribution into the droplet concentration.

[30] Equations (4) and (33)–(36) show the following. The lognormal size spectrum of the dry aerosol with the parameters described above is equivalent to the lognormal CCN activity spectrum by supersaturations $\varphi_s(s)$; that is, the shape is preserved under transformations between the radius and supersaturation variables. This feature is similar to that found in the work of *Abdul-Razzak et al.* [1998] and *Fountoukis and Nenes* [2005]. The difference of our model with these works is in that they assume soluble fraction proportional to the volume ($\beta = 0.5$), while our model for $\varphi_s(s)$ generalizes this expression and allows variable soluble fraction. For $\beta = 0.5$ (homogeneously mixed in volume), (35) for σ_s shows that the argument in the exponent (33) can be rewritten as $(-1/2)[(2/3)\ln(s/s_0)/\ln\sigma_d]^2$, which coincides with the cited works. For soluble fraction proportional to the surface, $\beta = 0$, as can be for the dust particles covered by the soluble film, the mean geometric supersaturation $s_0 \sim r_{d0}^{-1}$, and not $\sim r_{d0}^{-3/2}$, as in the case $\beta = 0.5$; the logarithm $\ln\sigma_s$ is

50 % smaller with $\beta = 0$, the argument becomes $(-1/2)[\ln(s/s_0)/\ln\sigma_d]^2$ and $\varphi_s(s)$ becomes much narrower. This means that the maximum in the activation spectrum is reached at another s_m and drop activation occurs over narrower s-range with $\beta = 0$.

4.3. Algebraic Differential CCN Spectrum

[31] An algebraic form of the differential activity spectrum can be obtained substituting $r_d(s)$ from (29) and $r_{d0}(s_0)$ from (34) into the conservation equation (32) with $f_d(r_d)$ from (24):

$$\varphi_s(s) = \frac{k_{s0}N_a}{s_0}\frac{(s/s_0)^{k_{s0}-1}}{\left[1 + (s/s_0)^{k_{s0}}\right]^2}, \qquad (37)$$

or, in a slightly different form that is more convenient for comparison with the other models

$$\varphi_s(s) = k_{s0}C_0 s^{k_{s0}-1}\left(1 + \eta_0 s^{k_{s0}}\right)^{-2}, \qquad (38)$$

Here

$$k_{s0} = \frac{4}{\sqrt{2\pi}\ln\sigma_s} = \frac{4}{\sqrt{2\pi}(1+\beta)\ln\sigma_d}, \qquad (39a)$$

$$C_0 = N_a s_0^{-k_{s0}} = N_a\left(\frac{27b}{4A_k^2}\right)^{k_{s0}/2}(r_{d0})^{k_{s0}(1+\beta)}, \qquad (39b)$$

$$\eta_0 = s_0^{-k_{s0}} = \left(\frac{27b}{4A_k^2}\right)^{k_{s0}/2}(r_{d0})^{k_{s0}(1+\beta)}. \qquad (39c)$$

(It is shown below that k_{s0} is the asymptotic value of the k-index in the CCN activity power law at small s). Expression (38) can be also obtained from the lognormal law (33) using the similarity relation (23), which again illustrates the equivalence of the lognormal and algebraic distributions.

[32] The first term, $k_{s0}C_0 s^{k_{s0}-1}$, on the right-hand side of (38) represents *Twomey*'s [1959] power law (2). In contrast to the C_0 and k_{s0} based on fits to experimental data, here the analytical dependence is derived from the Köhler's theory and algebraic approximation of the lognormal functions, and parameters C_0, k_{s0} are expressed directly via aerosol parameters. This first term describes drop activation at small supersaturations $s \ll s_0$ (as in the clouds with weak updrafts and in the "haze chambers") and grows with s as $s^{k_{s0}-1}$. The second term in parenthesis decreases at large $s \gg s_0$ as $s^{-2k_{s0}}$, overwhelms the growth of the first term, and ensures the asymptotic decrease $\varphi_s(s) \sim s^{-k_{s0}-1}$. Thus the term in parenthesis serves effectively as a correction to the Twomey law and prevents an unlimited growth of concentration of activated drops at large supersaturations.

[33] The entire CCN spectrum (38) resembles the corresponding equation from *Cohard et al.* [1998, 2000]:

$$\varphi_s(s) = kCs^{k-1}\left(1 + \eta s^2\right)^{-\lambda}, \qquad (40)$$

where the first term is also the Twomey's differential power law, and the term in parenthesis was added by the authors as
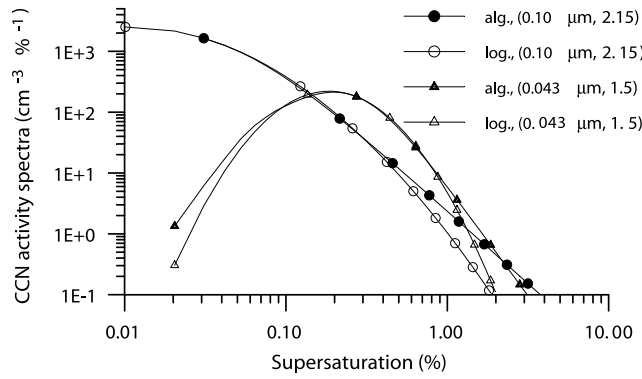
Figure 8. Comparison of the algebraic (alg.) and lognormal (log.) differential CCN activity spectra $\varphi_s(s)$. A pair of digits in the parentheses in the legend denotes modal radius r_m in μm and dispersion σ_d of the corresponding dry aerosol spectrum.

an empirical correction with the two parameters η, λ that were varied and chosen by fitting the experimental data. Thus the algebraic representation of $\varphi_s(s)$ (38) found here establishes a bridge between the Twomey's power law with its corrections as in the work of *Cohard et al.* [1998, 2000] and the lognormal parameterizations of drop activation as in the work of *Ghan et al.* [1993, 1995], *Abdul-Razzak et al.* [1998], *Abdul-Razzak and Ghan* [2000], and *Fountoukis and Nenes* [2005].

[34] Shown in Figure 7 is an example of the CCN differential activity spectrum $\varphi_s(s)$ (38) calculated with $b = 0.25$ (CCN with ~50 % of ammonium sulfate or ~20 % of NaCl) and four combinations of modal radii and dispersions. The area beneath each curve represents the drop concentration N_{dr} that could be activated at any given supersaturation s, so that the maximum of $\varphi_s(s)$ indicates the region of s where its increase leads to the most effective activation. A remarkable feature of this figure is a substantial sensitivity to the variations of r_m, σ_d. The maximum for the maritime-type spectrum with $r_m = 0.1$ μm, $\sigma_d = 2$ lies at very small $s \sim 0.01$ %. When σ_d decreases to 1.5 or r_m decreases to 0.03 (closer to the continental spectrum), the maximum of $\varphi_s(s)$ shifts to $s \sim 0.04-0.1$ %. With $r_m = 0.03$ μm, $\sigma_d = 1.5$, the region $s \sim 0.01-0.1\%$ becomes relatively inactive and the maximum shifts to 0.4%. Thus even moderate narrowing of the dry spectra or decrease in the modal radius may require much greater vertical velocities for activation of the drops with the same concentrations.

[35] A comparison of the algebraic (37) and lognormal (33) differential activity spectra in Figure 8 shows their general good agreement. The discrepancy increases in the both tails, but their contributions into the number density is small as will be illustrated below. Thus the algebraic functions (37), (38) approximate the lognormal spectrum (33) with good accuracy.

5. Droplet Concentration and Modified Power Law for Drops Activation

5.1. Droplet Concentration Based on the Lognormal and Algebraic CCN Spectra

[36] The concentration of CCN or activated drops can be obtained by integration of the differential activity spectrum

$\varphi_s(s)$ (33) over the supersaturations to the maximum value s reached in a cloudy parcel:

$$N_d(s) = N_{CCN}(s) = \int_0^s \varphi_s(s')ds' = \frac{N_a}{2}\left\{1 + erf\left(\frac{1}{\sqrt{2}}\frac{\ln(s/s_0)}{\ln\sigma_s}\right)\right\},$$

(41)

where s_0 and σ_s are defined by (34), (35). Equation (41) is similar to the corresponding expressions derived by *von der Emde and Wacker* [1993], *Ghan et al.* [1993, 1995], *Abdul-Razzak et al.* [1998], *Abdul-Razzak and Ghan* [2000], *Fountoukis and Nenes* [2005] that also arrive at *erf* function. A generalization of these works in (41) is the same as was discussed for the differential activation spectrum in previous section, in variable soluble fraction β, which is discussed below.

[37] Droplet or CCN concentration in algebraic form can be obtained now in two equivalent ways. The first way is integration of the algebraic CCN spectrum $\varphi_s(s)$ (37) or (38) over s:

$$N_{CCN}(s) = N_a\frac{(s/s_0)^{k_{s0}}}{\left[1 + (s/s_0)^{k_{s0}}\right]} = C_0 s^{k_{s0}}\left[1 + \eta_0 s^{k_{s0}}\right]^{-1},$$

(42)

where C_0 and η_0 are defined in (39b) and (39c). The second way is as in the work of *Ghan et al.* [1993] by substituting (21) for the equality of *erf* and *tanh* into (41), which also yields (42). The derivation of (41) and (42) along with equivalence (20), (21) emphasizes again the fact that differential CCN distributions by critical radii or supersaturations are smoothed Dirac delta functions, while their integrals, droplet concentrations, are smoothed Heaviside step functions.

[38] According to (42), the asymptotic of $N_{CCN}(s)$ at $s \ll s_0$ is the Twomey power law $N_{CCN}(s) = C_0 s^{k_{s0}}$. The term in parenthesis is a correction, its asymptote at $s \gg s_0$ is $s^{-k_{s0}}$, it compensates the growth of the first term and prevents unlimited drop concentration. The asymptotic limit of drop concentration is $N_{CCN}(s) \to N_a$ at large s, and hence the number of activated drops is limited by the total aerosol concentration.

[39] Equation (42) is similar to the corresponding equation from *Ghan et al.* [1993], but is expressed via supersaturation dispersion instead of the modal radius as in that work and is generalized here for the variable soluble fraction β, which causes the following difference. As follows from definitions of k_{s0} (39a), the power index k_{s0} differs by the factor $(1 + β)$ from the corresponding expression $k_{gh} = 4/(\sqrt{2\pi}\ln\sigma_d)$ in the work of *Ghan et al.* [1993], who assumed soluble fraction proportional to the volume, i.e., in our terms $β = 0.5$. With this value, $k_{s0} = (2/3)k_{gh}$, and the asymptotic of N_{CCN} for small s is $N_{CCN} \sim s^{k_{s0}} \sim s^{(2/3)k_{gh}}$, which coincides with the expression in the work of *Ghan et al.* [1993]. However, for $β = 0$ (surface-proportional soluble fraction), the index k_{s0} is 1.5 times higher than with $β = 0.5$, and, as mentioned before, the functions $N_{CCN}(s)$ increase (droplets activate) over much narrower interval of s.

[40] If the dry aerosol size spectrum is multimodal with I modes (e.g., $I = 3$ in a three-modal distributions [*Whitby*, 1978]), then it can be written as a superposition of I lognormal fractions (4) with N_{ai}, σ_{di}, and r_{d0i} being the number concentration, dispersion, and mean geometric radius of the ith fraction. The mean geometric supersaturations s_{0i}, dispersions σ_{si}, and the other parameters for each fraction are then defined by the same equations as described above for a single fraction. Then the algebraic dry and wet size spectra, the differential and integral activity spectra are obtained for each fraction as described above and the corresponding multimodal spectra are superpositions of the I fractions. The multimodal CCN activity spectrum in algebraic form is derived from (42):

$$N_d(s) = \sum_{i=1}^{I} N_{ai} \frac{(s/s_{0i})^{k_{s0i}}}{\left[1 + (s/s_{0i})^{k_{s0i}}\right]} = \sum_{i=1}^{I} C_{0i} s^{k_{s0i}} \left[1 + \eta_{0i} s^{k_{s0i}}\right]^{-1}.$$

(43)

Equation (43) for $\beta = 0.5$ is similar to the corresponding equation from *Ghan et al.* [1995] where $N_d(s)$ is expressed in terms of critical radii, but expresses it here directly via supersaturation and generalizes for the other β. The parameters β_i can be different for each fraction, e.g., $\beta_i = 0.5$ may correspond to the accumulation mode, and $\beta_i = 0$ may correspond to the coarse mode consisting of the dust particles coated with the soluble film.

5.2. Revived Power Law for the Drop Concentration, Power Index $k(s)$, and Coefficient $C(s)$

[41] The power law (1), $N_{CCN} = Cs^k$, is often used for parameterization of the results of CCN measurements and of drop activation in many cloud models. An analytical function for the k- index can be found now (similar to the μ-index (16)) using the method from *Khvorostyanov and Curry* [2002, 2005] for the power law representation of the continuous functions. Using (1) and its derivative $N'_{CCN}(s)$ (2) and solving these two equations for $k(s)$, we obtain:

$$k(s) = s \frac{N'_{CCN}(s)}{N_{CCN}(s)} = s \frac{\varphi_s(s)}{N_{CCN}(s)}$$

(44)

Equation (44) allows evaluation of $k(s)$ with known differential $\varphi_s(s)$ and cumulative $N_{CCN}(s)$ CCN spectra. Substituting here (33) for $\varphi_s(s)$ and (41) for $N_{CCN}(s)$, we obtain $k(s)$ in terms of lognormal functions:

$$k(s) = \sqrt{\frac{2}{\pi} \frac{1}{\ln \sigma_s}} \exp\left[-\frac{\ln^2 (s/s_0)}{2 \ln^2 \sigma_s}\right] \left[1 + erf\left(\frac{\ln(s/s_0)}{\sqrt{2} \ln \sigma_s}\right)\right]^{-1}.$$

(45)

Here s_0 and σ_s are defined by (34), (35). The algebraic form of the index $k(s)$ is obtained by substitution of (37) for $\varphi_s(s)$ and (42) for $N_{CCN}(s)$ into (44):

$$k(s) = k_{s0}\left[1 + (s/s_0)^{k_{s0}}\right]^{-1} = k_{s0}\left[1 + s^{k_{s0}} r_{d0}^{k_{s0}(1+\beta)} \left(\frac{27b}{4A_k^3}\right)^{k_{s0}/2}\right]^{-1}.$$

(46)

If the aerosol size spectrum is multimodal and is given by a superposition of I algebraic distributions, then the k-index is derived from (44), (43) by summation over I modes:

$$k(s) = \sum_{i=1}^{I} \frac{k_{s0i} N_{ai} (s/s_{0i})^{k_{s0i}}}{\left[1 + (s/s_{0i})^{k_{s0i}}\right]^2} \cdot \left\{\sum_{i=1}^{I} N_{ai} \frac{(s/s_{0i})^{k_{s0i}}}{\left[1 + (s/s_{0i})^{k_{s0i}}\right]}\right\}^{-1},$$

(47)

where the parameters k_{s0i}, s_{0i}, N_{ai} are defined as before but for each ith mode.

[42] Equations (45)–(47) allow evaluation of $k(s)$ for any s with given σ_s and s_0 that are expressed via r_d, σ_d, b, and β. That is, knowledge of the size spectra and composition of the dry or wet CCN allows direct evaluation of $k(s)$ over the entire s-range. This solves the problem outlined in *Jiusto and Lala* [1981], *Yum and Hudson* [2001] and many other studies: various values of the k-index at various s. Equations (45)–(47) provide a continuous representation of k over the entire s-range. Note that the k-index is not constant for a given air mass or aerosol type but depends on a given s, at which it is measured. Equation (46) shows that for $s \ll s_0$, the asymptotic value $k(s) = k_{s0}$. For $s \gg s_0$, the index decreases with s as $k(s) = k_{s0}(s/s_0)^{-k_{s0}}$ and tends to zero. This behavior is in agreement with the experimental data from *Jiusto and Lala* [1981], *Yum and Hudson* [2001], and others.

[43] The coefficient $C(s)$ can be now calculated using (42) for $N_{CCN}(s)$ and (46) for $k(s)$

$$C(s) = N_{CCN}(s) s^{-k(s)} = C_0 s^{\chi(s)} \left[1 + (s/s_0)^{k_{s0}}\right]^{-1},$$

(48)

where C_0 is defined in (39b). The power index $\chi(s)$ of s in (48) is

$$\chi(s) = k_{s0} - k(s) = k_{s0} \frac{(s/s_0)^{k_{s0}}}{1 + (s/s_0)^{k_{s0}}}.$$

(49)

Now we can write the CCN (or droplet) concentration in the form of a modified power law

$$N_{CCN}(s) = C(s) s^{k(s)}, \quad s \text{ in share of unit.}$$

(50)

This equation is usually used with supersaturation s in percent, related to s_{su} in share of unit as $s = 10^{-2} s_{su}$. Substitution of this relation into (50) yields a more conventional form

$$N_{CCN}(s) = C_{pc}(s) s^{k(s)}, \quad s \text{ in percent.}$$

(51)

In (51), both $k(s)$ and $C(s)$ depend on the ratio s/s_0 and thus do not depend on units; $k(s)$ is calculated again from (46) but with s and s_0 in percent, and the coefficient

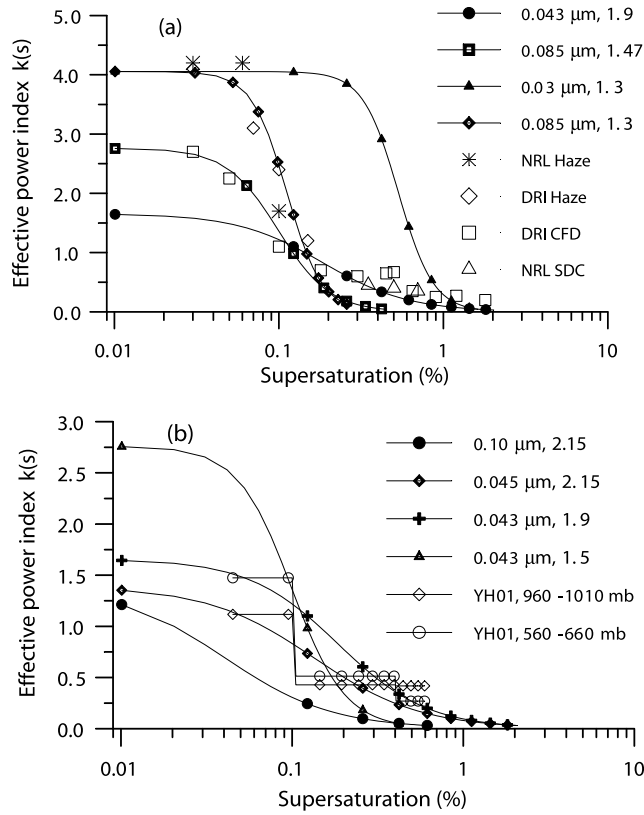$$C_{pc}(s_{pc}) = 10^{-2k(s)} C(s).$$

(52)

Figure 9. Supersaturation dependence of the k-index calculated for the lognormal size spectrum of dry CCN with various modal radii r_m and dispersions σ_d indicated in the legend and comparison: (a) with the experimental data from *Jiusto and Lala* [1981] from four chambers (haze chamber; continuous flow diffusion chamber, CFD; and static diffusion chamber, SDC), and (b) with the data collected in FIRE-ACE in 1998 [*Yum and Hudson*, 2001, hereinafter referred to as YH01] at the heights $960-1010$ mb and $560-660$ mb.

Equation (51) is similar to (1), however, now with the parameters depending on s as just described. Hence $k(s)$ and $C(s)$ are now expressed directly via the parameters of the lognormal spectrum (N_a, r_{d0}, σ_d) and its physicochemical properties via simple parameterization of b in (9a)–(9c).

[44] Finally, the power law for the multimodal aerosol types is described again by (50), (51) with the $k(s)$-index evaluated from (47) and the coefficient $C(s)$

$$C(s) = \sum_{i=1}^{I} C_{0i} s^{\chi_i(s)} \left[1 + (s/s_{0i})^{k_{s0i}} \right]^{-1}, \qquad (53)$$

where $\chi_i = k_{s0i} - k(s)$, and k_{s0i}, C_{0i}, s_{0i}, N_{ai} are defined for each ith mode. The coefficient $C_{pc}(s)$ with supersaturation in percent is defined by (52). The number of modes I is determined by the nature of aerosol and is the same as used for multimodal size spectra with the lognormal approach in the work of *Ghan et al.* [1995], *Abdul-Razzak and Ghan* [2000], and *Fountoukis and Nenes* [2005].

[45] This analytical s-dependence of C and k in (50), (51) provides a theoretical basis for many previous findings and

improvements of the drop activation power law. In particular, the C-k space constructed by *Braham* [1976] based on experimental data follows now from the equations for $k(s)$ and $C(s)$ with use of any relation of maximum s to vertical velocity. The decrease of the k-slopes with increasing s analyzed by *Jiusto and Lala* [1981], *Yum and Hudson* [2001], *Cohard et al.* [1998, 2000], and many others is predicted by (45)–(47), as well as its dependence on the nature of aerosol. The proportionality of coefficient C to the aerosol concentration explains substantially greater values of C observed in continental than in maritime air masses as compiled by *Twomey and Wojciechowski* [1969] and *Hegg and Hobbs* [1992] and used by cloud modelers.

5.3. Supersaturation Dependence of $k(s)$, $C(s)$, and $N_d(s)$

[46] The equivalent power index $k(s)$ calculated with (46) and a monomodal lognormal size spectrum is shown in Figures 9a and 9b and is compared with the experimental data from *Jiusto and Lala* [1981], who collected the data from several chambers and to the field data collected by *Yum and Hudson* [2001] with a continuous flow diffusion chamber (CFD) at two altitudes in the Arctic in May 1998 during the First International Regional Experiment-Arctic Cloud Experiment (FIRE-ACE). It is seen that the k-index is not constant as assumed in many cloud models. The calculated k-indices reach the largest values of $1.5-4.2$ at $s \leq 0.01$ %, where it tends to the asymptotic k_{s0} (39a) and increases with decreasing dispersion of the dry CCN spectrum since $k_{s0} \sim (\ln\sigma_d)^{-1}$. As s increases, $k(s)$ is initially almost constant, then decreases slowly up to $s \sim 0.03-0.05\%$ and then decreases more rapidly in the region $s \sim 0.05-0.12\%$ to values less than $0.1-0.2$ at $s > 1\%$. The k-indices increase with decreasing modal radii and dispersions. Agreement of calculated $k(s)$ with haze chamber data is reached at $\sigma_d = 1.3$, $r_d = 0.085$ μm, and with CFD at $\sigma_d = 1.5$, $r_d = 0.043$ μm. Agreement with the Arctic field data by *Yum and Hudson* [2001] is reached with $r_m = 0.045$ μm, $\sigma_d = 2.15$ in the layer $960-1010$ mb and $r_m = 0.043$ μm, $\sigma_d = 1.9$ in the layer $560-660$ mb.

[47] Thus this model explains and describes quantitatively the observed decrease in the k-index with increasing supersaturation reported previously by many investigators (e.g., *Twomey and Wojciechowski*, [1969], *Braham* [1976], *Jiusto and Lala* [1981]; see review in PK97) and relates it to the aerosol size spectra. A more detailed analysis of experimental data with these equations should be based on simultaneous use of the measured multimodal aerosol size spectra and CCN supersaturation activity spectra.

[48] In contrast to most models where both k and C are constant and to some other models where the k-index depends on s, but the coefficient C is constant [e.g., *Cohard et al.*, 1998, 2000], the values of "effective" $C(s)$, $C_{pc}(s)$ in this model also depend on supersaturation. The spectral behavior of $C_{pc}(s)$ calculated from (52) with different r_m, σ_d and the same $N_a = 100$ cm^{-3} is shown in Figure 10. For $s \ll s_0$, the coefficients tend to the asymptotic limit $C_{pc}(0) = 10^{-2k_{s0}}C_0$ and reach values of 10^3-10^5 cm^{-3} caused by the dependence $C_0 \sim A_k^{-2k_{s0}} r_{d0}^{k_{s0}(1+\beta)}$ with $A_k \sim 10^{-7}$ cm and $r_{d0} \sim 3 \times 10^{-6}$ to 10^{-5} cm. This dependence causes increase in C_{pc} with decreasing σ_d (increasing k_{s0}) and with increasing r_{d0} seen at small s in Figure 10; i.e., the narrower spectra and the larger modal radius, the faster drop activation at
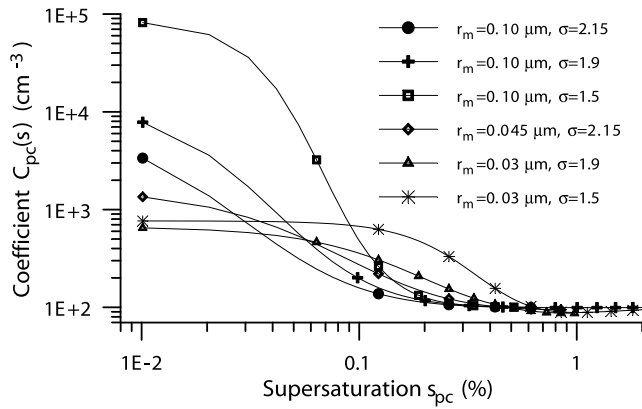
Figure 10. Equivalent coefficient $C_{pc}(s)$ in the power law for N_{CCN} calculated for the lognormal size spectrum of dry CCN with modal radii r_m and dispersions σ_d indicated in the legend and other parameters described in the text. For the convenience of comparison, all curves are calculated with $N_a = 10^2$ cm^{-3}.

small s. The values of $C_{pc}(s)$ decrease with increasing s by 1–3 orders of magnitude and tend to N_a at $s_{pc} > 0.1$–0.7%, since the asymptotics at large s is $C_{pc}(s_{pc}) = 10^{-2k(s)}N_a s_{pc}^{-k(s)}$, and $k(s) \to 0$ at large s, hence all $C_{pc} \to N_a$ at $s_{pc} \geq 0.5\%$ as seen in Figure 10. Thus $N_{CCN}(s) = C_{pc}s^{k(s)} \sim 10^{-2k(s)}N_a$ and tends to the limiting value N_a, which ensures finite values of N_a in contrast to the models with constant k, C.

[49] A comparison of the concentrations $N_{CCN}(s)$ calculated using the power law (51) and *erf* function (41) shows in Figure 11 their good agreement and illustrates good accuracy of the algebraic distributions and renewed power law as compared to the direct integration of the lognormal distributions. The curves $N_{CCN}(s)$ calculated with the newer power law are not linear in log-log coordinates as it is with (1) and constant C_0, k, but are concave in agreement with the measurements [e.g., *Jiusto and Lala*, 1981; *Hudson*,

1984; *Yum and Hudson*, 2001] and other models [e.g., *Ghan et al.*, 1993, 1995; *Feingold et al.*, 1994; *Cohard et al.*, 1998, 2000]. The reason for this concavity is quite clear from Figures 6–8 for the size and activity spectra: the rate of increase in concentration of activated drops $dN_d(s)/ds$ is greatest at small supersaturations in the left branch of $\varphi_s(s)$ (Figures 7 and 8), or in the right branch of $f_d(r_d)$ at $r_d > r_m$ (Figure 6), then $dN_d(s)/ds$ decreases with growing s, especially at $s > 1\%$, i.e., in the left branch of the small dry CCN with $r_d < 0.03$ μm (Figure 6). Effectively, some "saturation" with respect to supersaturation occurs, causing $k(s)$, $C(s)$ and $dN_d(s)/ds$ to decrease with s and leading to finite $N_d(s)$ at large s.

[50] Finally, Figure 12 shows $N_{CCN}(s)$ calculated with the lognormal size spectra and compared to the corresponding field data obtained by *Yum and Hudson* [2001] in the FIRE-ACE campaign in May 1998 in the Arctic. The parameters r_m, σ_d, and N_a were varied slightly in the calculations, although we constrained the calculations to the measured k-indices (Figure 10b), so that the values of the parameters had to provide an agreement for both $k(s)$ and $N_{CCN}(s)$. Good agreement over the entire range of supersaturations was found with the values indicated in the legend. The values of modal radii and dispersions are typical for the accumulation mode. This comparison shows that this model of the power law can reasonably reproduce the experimental data on CCN activity spectra and concentrations of activated drops and can be used for parameterization of drop activation in cloud models.

6. Summary and Conclusions

[51] A model of the lognormal size spectrum of mixed (partially soluble) dry CCN with parameterization of the soluble fraction as a function of the dry nucleus radius is used to consider the processes of humidity transformation of the dry size spectrum into the spectrum of the wet interstitial aerosol and drop activation. Using the expressions for the radius of a solution particle as a function of relative humidity, it was shown that a lognormal size spectrum of
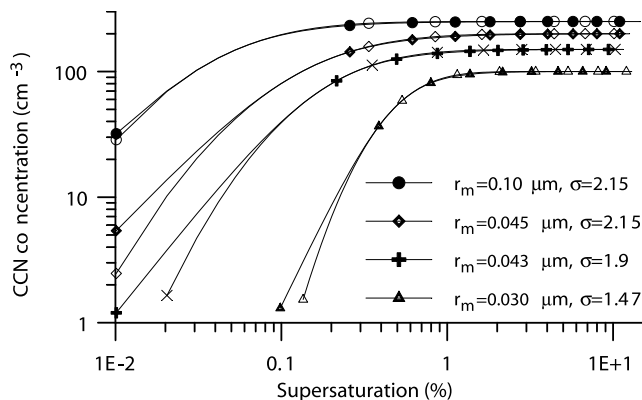

Figure 11. Comparison of the accumulated CCN spectra $N_{CCN}(s)$ calculated using power law equation (51) (solid symbols) and using (41) with *erf* function (open symbols). The values of the corresponding modal radii r_m and dispersions σ_d of the dry aerosol spectra are indicated in the legend. For convenience of comparison, N_{CCN} is calculated with the dry aerosol concentrations of 250, 200, 150, and 100 cm^{-3} from the upper to lower curves.

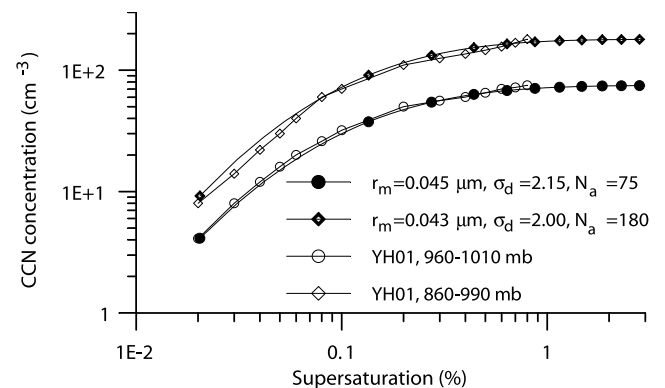**Figure 12.** Supersaturation dependence of the CCN integral activity spectrum $N_{CCN}(s)$ calculated with the new power law (51) for the lognormal size spectra with r_m, σ_d and N_a (in cm^{-3}) indicated in the legend (solid rhombs and circles), compared to the corresponding field data obtained by *Yum and Hudson* [2001] in FIRE-ACE campaign in May 1998 in the Arctic (open rhombs and circles).

the dry aerosol transforms into the lognormal spectra of the cloud interstitial aerosol at supersaturation. The mean geometric radii and dispersions of these spectra are expressed via the corresponding parameters of the dry aerosol. A quasi-power law Junge-type representation of the lognormal spectra was derived, and corresponding power indices and coefficients are expressed via the corresponding mean geometric sizes and dispersions of the dry and interstitial aerosol. Using various representations of the smoothed Dirac delta function, an algebraic equivalent was found for the lognormal dry and interstitial aerosol size spectra. These algebraic representations allow simplification of analytical estimations and evaluation of various moments of the spectra such as condensation rate, etc.

[52] On the basis of Köhler theory, the differential CCN activity spectrum is expressed in lognormal form for various soluble fractions. This spectrum coincides with the previous parameterizations from *Abdul-Razzak et al.* [1998] and *Fountoukis and Nenes* [2005] for soluble fraction proportional to the particle volume and generalizes them for other soluble fractions (e.g., soluble fraction proportional to surface area as can be for the insoluble dust particles coated with a thin soluble shell). The algebraic equivalent of the lognormal differential CCN activity spectra is found, $\varphi_s(s) = k_{s0}C_0 s^{k_{s0}-1}(1 + \eta_0 s^{k_{s0}})^{-2}$. This is a generalization and correction of the Twomey's differential activity spectrum: the first term is Twomey's power law, and the term in parentheses ensures finite droplet concentrations at high supersaturations. The functional form of this activity spectra is similar to the empirical correction by *Cohard et al.* [1998, 2000] of Twomey's power law but differs from these works by the analytical dependence that leads to the simple algebraic expressions for the droplet concentration, and the three parameters C_0, k_{s0}, η_0 of this spectrum are directly expressed via the size parameters and composition of the dry aerosol.

[53] The cumulative CCN activity spectrum, $N_{CCN}(s)$ is found in lognormal form, which coincides with the previous parameterizations by *von der Emde and Wacker* [1993], *Ghan et al.* [1993, 1995], *Abdul-Razzak et al.* [1998], and *Fountoukis and Nenes* [2005] for the soluble fraction proportional to the particle volume (homogeneously mixed particles). We have generalized the previous lognormal parameterizations for other soluble fractions, in particular, for the soluble fraction proportional to the particle surface, as, e.g., for dust or other insoluble particles with soluble coatings on the surface [*Levin et al.*, 1996; *Bauer and Koch*, 2005]. It is shown that the algebraic form of the cumulative CCN spectrum, $N_{CCN}(s)$, as found in the work of *Ghan et al.* [1993] from the lognormal spectrum using the equivalence of *erf* and *tanh*, can be obtained also by integration of the algebraic differential spectrum $\varphi_s(s)$. This establishes a bridge and illustrates the relation among the numerous approaches based on the differential power law or algebraic CCN spectra, and those that derive $N_{CCN}(s)$ by direct integration of lognormal aerosol size spectra using the Köhler relation between the critical radius and supersaturation.

[54] A modified power law is derived for the drop activation, $N_{CCN}(s) = C(s)s^{k(s)}$. The modified power law yields drop concentration limited by the total aerosol number, in contrast to the previous power law with unlimited $N_{CCN}(s)$ at high supersaturations. Algebraic formulae are found for $C(s)$, and $k(s)$ as continuous functions of

supersaturation s, which correctly describe their decrease with s, i.e., predict the observed concave $N_{CCN}(s)$ spectra. The new formulation expresses $C(s)$ and $k(s)$ via parameters of the dry aerosol spectrum (the modal radius, dispersion, and aerosol concentration) and the physicochemical properties of the aerosol and the distribution of the soluble fraction in the aerosol particles. The derivation of the new power law for the CCN activity spectrum clearly shows its equivalence and correspondence to the lognormal parameterizations. The modified power law permits using the wealth of the data on the C, k parameters accumulated over this time. Additionally, the C, k parameters can be directly calculated based on the aerosol microstructure and recalculated from $s = 1\%$ to any s. The C-k space suggested by *Braham* [1976] based on experimental data can now be obtained from calculations using aerosol microstructure as the input.

[55] The relationships derived here for CCN concentration and activity spectra can be easily incorporated into cloud and climate models. Relative to the lognormal parameterization that is included in climate models [*Ghan et al.*, 1997; *Lohmann et al.*, 1999; *Nenes and Seinfeld*, 2003], the parameterizations presented here include an additional element of necessary physics, related to the treatment of the soluble fraction and how the aerosol particles are mixed. An additional advantage of the new parameterizations is their algebraic and computational simplicity, allowing for simple analytical determination of derivatives and higher order moments. Further, the power law and algebraic representations are easily superimposed to represent multimodal spectra.

Notation

A_k	the Kelvin curvature parameter.
$B = br_d^{2(1+\beta)}$	the nucleus activity.
b	the parameter defined in (9a), (9b), (9c) that describes the soluble fraction of an aerosol particle.
C	the coefficient in the power law for integral CCN activity spectrum.
C_0	the coefficient in the differential power law CCN activity spectrum (38).
c_1, c_2	the coefficients defined in (30) and (32a).
c_f	the coefficient in the Junge-type size spectrum.
$f(r)$	the general notation for the aerosol size spectrum.
$f_d(r_d)$, $f_w(r_w)$	the size distribution functions of the dry and wet aerosol.
H, H_{th}	the relative humidity and the threshold of deliquescence of the soluble fraction.
k	the index in the power law for integral CCN activity spectrum.
k_0	the parameter of algebraic size spectra.
k_{0d} and k_{0w}	the parameters of the dry and wet algebraic size spectra.
k_1, k_2	the indices defined in (30) and (32a).
k_{s0}	the power index of the algebraic supersaturation spectrum.

l_0	the thickness of the soluble shell on an insoluble aerosol particle.
M_w and M_s	the molecular weights of water and aerosol soluble fraction.
m_s	the mass of the soluble fraction of an aerosol particle.
N_a	the aerosol number concentration.
N_{CCN}	the concentration of the cloud condensation nuclei (CCN).
N_d	the droplet number concentration.
R	the universal gas constant.
$r_b = 2A_k/3s$	the boundary radius of interstitial CCN.
r_{cr}	the CCN critical radius of drop activation.
r_d	the radius of a dry aerosol particle.
r_{d0}	the mean geometric radius of the dry aerosol spectrum.
r_{d1}	the scaling parameter in (9b).
r_m	the modal radius of the aerosol size spectrum.
$r_w(H)$	the radius of a wet particle.
r_{w0}	the wet mean geometric radius.
$s = (\rho_v - \rho_{vs})/\rho_{vs}$	the supersaturation.
s_0	the mean geometric supersaturation.
s_m	the modal supersaturation.
T	the temperature (in degrees Kelvin).
α	the parameter of width in the smoothed Dirac delta function.
β	the power index defined in (8) that describes the soluble fraction of an aerosol particle.
χ	the power index of s in the coefficient $C(s)$ in (48).
$\delta(x)$	Dirac's delta function.
ε_v	the volume fraction of the soluble fraction.
ε_{v0}	the reference soluble fraction.
Φ_s	the osmotic potential.
$\varphi_s(s)$	differential CCN activity spectrum.
η	the parameter of the differential activity spectrum in (39c).
μ	the power index of Junge-type power law spectrum $\sim r^{-\mu}$.
ν	the number of ions in solution.
ρ_v, ρ_{vs} and ρ_w	the densities of vapor, saturated vapor and water.
ρ_s	the density of the soluble fraction.
σ_d	the dispersion of the dry spectrum.
σ_s	the supersaturation dispersion.
σ_w	the dispersion of the wet aerosol size spectrum.
ζ_{sa}	the surface tension at the solution-air interface.

References

Abdul-Razzak, H., and S. J. Ghan (2000), A parameterization of aerosol activation: 2. Multiple aerosol types, *J. Geophys. Res.*, *105*, 6837–6844.

Abdul-Razzak, H., S. J. Ghan, and C. Rivera-Carpio (1998), A parameterization of aerosol activation: 1. Single aerosol type, *J. Geophys. Res.*, *103*, 6123–6131.

Albrecht, B. (1989), Aerosols, cloud microphysics and fractional cloudiness, *Science*, *245*, 1227–1230.

Bauer, S. E., and D. Koch (2005), Impact of heterogeneous sulfate formation at mineral dust surfaces on aerosol loads and radiative forcing in the GISS GCM, *J. Geophys. Res.*, *110*, D17202, doi:10.1029/2005JD005870.

Braham, R. R. (1976), CCN spectra in c-k space, *J. Atmos. Sci.*, *33*, 343–346.

Cohard, J.-M., J.-P. Pinty, and C. Bedos (1998), Extending Twomey's analytical estimate of nucleated cloud droplet concentrations from CCN spectra, *J. Atmos. Sci.*, *55*, 3348–3357.

Cohard, J.-M., J.-P. Pinty, and K. Suhre (2000), On the parameterization of activation spectra from cloud condensation nuclei microphysical properties, *J. Geophys. Res.*, *105*(D9), 11,753–11,766.

Feingold, G., B. Stevens, W. R. Cotton, and R. L. Walko (1994), An explicit cloud microphysics/LES model designed to simulate the Twomey effect, *Atmos. Res.*, *33*, 207–233.

Fitzgerald, J. W. (1975), Approximation formulas for the equilibrium size of an aerosol particle as function of its dry size and composition and ambient relative humidity, *J. Appl. Meteorol.*, *14*, 1044–1049.

Fitzgerald, J. W., W. A. Hoppel, and M. A. Vietty (1982), The size and scattering coefficient of urban aerosol particles at Washington D.C. as a function of relative humidity, *J. Atmos. Sci.*, *39*, 1838–1852.

Fountoukis, C., and A. Nenes (2005), Continued development of a cloud droplet formation parameterization for global climate models, *J. Geophys. Res.*, *110*, D11212, doi:10.1029/2004JD005591.

Ghan, S., C. Chuang, and J. Penner (1993), A parameterization of cloud droplet nucleation. part 1, Single aerosol species, *Atmos. Res.*, *30*, 197–222.

Ghan, S., C. Chuang, R. Easter, and J. Penner (1995), A parameterization of cloud droplet nucleation. 2, Multiple aerosol types, *Atmos. Res.*, *36*, 39–54.

Ghan, S., L. Leung, R. Easter, and H. Abdul-Razzak (1997), Prediction of cloud droplet number in a general circulation model, *J. Geophys. Res.*, *102*, 777–794.

Hänel, G. (1976), The properties of atmospheric aerosol particles as functions of the relative humidity at thermodynamic equilibrium with the surrounding moist air, *Adv. Geophys.*, *19*, 73–188.

Hegg, D. A., and P. V. Hobbs (1992), Cloud condensation nuclei in the marine atmosphere: A review, in *Nucleation and Atmospheric Aerosols*, edited by N. Fukuta and P. E. Wagner, pp. 181–192, A. Deepak, Hampton, Va.

Hudson, J. G. (1984), Cloud condensation nuclei measurements within clouds, *J. Clim. Appl. Meteorol.*, *23*, 42–51.

Ji, Q., and G. E. Shaw (1998), On supersaturation spectrum and size distribution of cloud condensation nuclei, *Geophys. Res. Lett.*, *25*, 1903–1906.

Jiusto, J. E., and G. G. Lala (1981), CCN-supersaturation spectra slopes (k), *J. Rech. Atmos.*, *15*, 303–311.

Junge, C. E. (1963), *Air Chemistry and Radioactivity*, 424 pp., Elsevier, New York.

Khvorostyanov, V. I., and J. A. Curry (1999a), A simple analytical model of aerosol properties with account for hygroscopic growth: 1. Equilibrium size spectra and CCN activity spectra, *J. Geophys. Res.*, *104*, 2163–2174.

Khvorostyanov, V. I., and J. A. Curry (1999b), A simple analytical model of aerosol properties with account for hygroscopic growth: 2. Scattering and absorption coefficients, *J. Geophys. Res.*, *104*, 2175–2184.

Khvorostyanov, V. I., and J. A. Curry (2002), Terminal velocities of droplets and crystals: power laws with continuous parameters over the size spectrum, *J. Atmos. Sci.*, *59*, 1872–1884.

Khvorostyanov, V. I., and J. A. Curry (2005), Fall velocities of hydrometeors in the atmosphere: Refinements to a continuous analytical power law, *J. Atmos. Sci.*, *62*, 4343–4357.

Korn, G. A., and T. M. Korn (1968), *Mathematical Handbook for Scientists and Engineers*, 831 pp., McGraw-Hill, New York.

Laktionov, A. G. (1972), Fraction of soluble in water substances in the particles of atmospheric aerosol, *Izv. Acad. Sci. USSR, Atmos. Oceanic Phys.*, Engl. Transl., *8*, 389–395.

Levich, V. G. (1969), *The Course of Theoretical Physics*, vol. 1, 910 pp., Nauka, Moscow.

Levin, L. M., and Y. S. Sedunov (1966), A theoretical model of condensation nuclei. The mechanism of cloud formation in clouds, *J. Rech. Atmos.*, *2*, 2–3.

Levin, Z., E. Ganor, and V. Gladstein (1996), The effects of desert particles coated with sulfate on rain formation in the eastern Mediterranean, *J. Appl. Meteorol.*, *35*, 1511–1523.

Lohmann, U., J. Feichter, C. C. Chuang, and J. E. Penner (1999), Predicting the number of cloud droplets in the ECHAM GCM, *J. Geophys. Res.*, *104*, 9169–9198.

Nenes, A., and J. H. Seinfeld (2003), Parameterization of cloud droplet formation in global climate models, *J. Geophys. Res.*, *108*(D14), 4415, doi:10.1029/2002JD002911.

Pruppacher, H. R., and J. D. Klett (1997), *Microphysics of Clouds and Precipitation*, 2nd ed., 954 pp., Springer, New York.

Rissman, T. A., A. Nenes, and J. H. Seinfeld (2004), Chemical amplification (or dampening) of the Twomey effect: Conditions derived from droplet activation theory, *J. Atmos. Sci.*, *61*, 919–930.

Sassen, K. P. J. DeMott, J. M. Prospero, and M. R. Poellot (2003), Saharan dust storms and indirect aerosol effects on clouds: CRYSTAL-FACE results, *Geophys. Res. Lett.*, *30*(12), 1633, doi:10.1029/2003GL017371.

Sedunov, Y. S. (1974), *Physics of Drop Formation in the Atmosphere*, translated from Russian by D. Lederman, 234 pp., John Wiley, Hoboken, N. J.

Seinfeld, J. H., and S. N. Pandis (1998), *Atmospheric Chemistry and Physics*, 1326 pp., John Wiley, Hoboken, N. J.

Smirnov, V. I. (1978), On the equilibrium sizes and size spectra of aerosol particles in a humid atmosphere, *Izv. Acad. Sci. USSR, Atmos. Oceanic Phys.*, *14*, 1102–1106.

Squires, P. (1958), The microstructure and colloidal stability of warm clouds, II, The causes of the variations of microstructure, *Tellus*, *10*, 262–271.

Twomey, S. (1959), The nuclei of natural cloud formation. II. The supersaturation in natural clouds and the variation of cloud droplet concentration, *Pure Appl. Geophys.*, *43*, 243–249.

Twomey, S. (1977), *Atmospheric Aerosols*, 302 pp., Elsevier, New York.

Twomey, S., and T. A. Wojciechowski (1969), Observations of the geographical variations of cloud nuclei, *J. Atmos. Sci.*, *26*, 684–696, 1969.

von der Emde, K., and U. Wacker (1993), Comments on the relationship between aserosol size spectra, equilibrium drop size spectra and CCN spectra, *Contrib. Atmos. Phys.*, *66*, 157–162.

Whitby, K. (1978), The physical characteristics of sulfur aerosols, *Atmos. Environ.*, *12*, 135–159.

Yum, S. S., and J. G. Hudson (2001), Vertical distributions of cloud condensation nuclei spectra over the springtime Arctic Ocean, *J. Geophys. Res.*, *106*, 15,045–15,052.

————————————

J. A. Curry, School of Earth and Atmospheric Sciences, Georgia Institute of Technology, 311 Ferst Drive, Atlanta, GA 30332-0340, USA. (curryja@eas.gatech.edu)

V. I. Khvorostyanov, Central Aerological Observatory, 3, Pervomayskaya str., Dolgoprudny, Moscow Region, 141700, Russia. (vitally.kh@g23.relcom.ru)